TISSUE ENGINEERING: Part A
Volume 18, Numbers 11 and 12, 2012

DOI: 10.1089/ten.tea.2011.0543

Direct Human Cartilage Repair Using Three-Dimensional Bioprinting Technology

Xiaofeng Cui, Ph.D.,[1,2] Kurt Breitenkamp, Ph.D.,[3] M.G. Finn, Ph.D.,[3]
Martin Lotz, M.D.,[1] and Darryl D. D'Lima, M.D., Ph.D.[1,2]

Current cartilage tissue engineering strategies cannot as yet fabricate new tissue that is indistinguishable from native cartilage with respect to zonal organization, extracellular matrix composition, and mechanical properties. Integration of implants with surrounding native tissues is crucial for long-term stability and enhanced functionality. In this study, we developed a bioprinting system with simultaneous photopolymerization capable for three-dimensional (3D) cartilage tissue engineering. Poly(ethylene glycol) dimethacrylate (PEGDMA) with human chondrocytes were printed to repair defects in osteochondral plugs (3D biopaper) in layer-by-layer assembly. Compressive modulus of printed PEGDMA was 395.73 ± 80.40 kPa, which was close to the range of the properties of native human articular cartilage. Printed human chondrocytes maintained the initially deposited positions due to simultaneous photopolymerization of surrounded biomaterial scaffold, which is ideal in precise cell distribution for anatomic cartilage engineering. Viability of printed human chondrocytes increased 26% in simultaneous polymerization than polymerized after printing. Printed cartilage implant attached firmly with surrounding tissue and greater proteoglycan deposition was observed at the interface of implant and native cartilage in Safranin-O staining. This is consistent with the enhanced interface failure strength during the culture assessed by push-out testing. Printed cartilage in 3D biopaper had elevated glycosaminoglycan (GAG) content comparing to that without biopaper when normalized to DNA. These observations were consistent with gene expression results. This study indicates the importance of direct cartilage repair and promising anatomic cartilage engineering using 3D bioprinting technology.

Introduction

Cartilage defects resulting from osteoarthritis, aging, and joint injury are a major cause of joint pain and chronic disability.[1] Without blood vessels, nerves, and lymphatics, mature cartilage cannot heal spontaneously. The most common treatment for advanced cartilage degeneration is joint replacement surgery, but this procedure is highly invasive, complicated, and expensive.[2] Although cell transplantation-based tissue engineering treatment for human cartilage repair was introduced almost two decades ago,[3] current cartilage tissue engineering strategies cannot as yet fabricate new tissue that is indistinguishable from native cartilage with respect to zonal organization, extracellular matrix (ECM) composition, and mechanical properties.[4] Furthermore, almost all current strategies of knee cartilage repair involve a procedure of removing healthy cartilage tissue around the lesion site to create artificial defects for further treatment or implantation.[5] This procedure in fact causes additional necrosis to the existing cartilage tissue and it is believed to lead to ultimate cartilage degeneration and failure of implanted tissue.[6]

Direct cartilage repair with engineered tissue closely mimicking native cartilage to the site of the lesion without any additional damage to the existing healthy tissue is therefore very attractive. The ideal implanted tissue is expected to integrate with existing native cartilage and to repair lesions of different sizes and thicknesses. The multifaceted nature of this challenge requires a technique adaptable to variable physical dimensions and properties for tissue repair; we believe that bioprinting technology, based on inkjet printing, provides the necessary capabilities.

Inkjet printing is a noncontact printing technique that reproduces digital pattern information onto a substrate with tiny ink drops.[7] Air bubbles generated by heating in the printhead collapse to provide pressure pulses to eject ink drops with various volumes from 10 to 150 pL.[8,9] Although the heating element in each nozzle raises the local temperature to 300°C and lasts for a few microseconds[10] during printing, ejected mammalian cells are heated for only 2 μs with a temperature rise of 4°C–10°C above ambient and an average cell viability of 90%.[11] With advantages of high-throughput digital control and highly accurate placement of cells, biological factors, and biomaterial scaffolds, functional

[1]Department of Molecular and Experimental Medicine, The Scripps Research Institute, La Jolla, California.
[2]Shiley Center for Orthopaedic Research and Education at Scripps Clinic, La Jolla, California.
[3]Department of Chemistry and The Skaggs Institute for Chemical Biology, The Scripps Research Institute, La Jolla, California.

human microvasculature for thick and complex tissues have been successfully fabricated using bioprinting.[12] Transient cell membrane pores developed during printing were also utilized for efficient gene transfection with minimum toxicity to cells.[11]

The typical production of biomaterial scaffolds usually involves the ejection of less viscous bioink onto more viscous biopaper. For example, collagen scaffold can be printed at 4°C and physically crosslinked at elevated temperature.[13] Alginate[14] and fibrin[12,15] scaffolds have been generated by printing the bioink (cells suspended in crosslinker) onto viscous biopaper substrate (uncrosslinked sodium alginate or fibrinogen) to fabricate two-dimensional (2D) or 3D patterns. These printed scaffolds have limited mechanical properties because of the nature of materials and crosslinking, and the crucial phenomenon of integration with native tissues directly is difficult. Therefore, a biocompatible and directly printable biomaterial scaffold that is capable of simultaneous polymerization during printing with mechanical properties matched to native tissue is critical for cartilage engineering.

Synthetic hydrogels formulated from poly(ethylene glycol) (PEG) macromers have been demonstrated to maintain chondrocyte viability and induce ECM deposition in proteoglycans and type II collagen.[16,17] The compressive modulus of PEG hydrogel is tunable to match that of human cartilage.[18] In addition, PEG is water soluble with low viscosity and can be modified to be photocrosslinkable, which makes it attractive for direct printing with simultaneous polymerization during printing. In this study, a Hewlett-Packard (HP) Deskjet 500 thermal inkjet printer was modified to precisely deposit human articular chondrocytes and poly(ethylene glycol) dimethacrylate (PEGDMA; MW, 3400) layer by layer into a cartilage defect within an osteochondral (OC) plug (3D biopaper) for cartilage repair. The objective of this study was to test the feasibility of bioprinting to precisely deliver cells and biomaterial scaffold to targeted 3D location in layer-by-layer assembly, and represents the first application of thermal inkjet-based bioprinting technology to the engineering of cartilage. The criteria for success were to control placement of individual cells, preserve cell viability, maintain chondrogenic phenotype, and demonstrate integration with host tissue, all of which were met.

Materials and Methods

Materials

Dulbecco's modified Eagle's medium (DMEM) was obtained from Mediatech (Manassas, VA). LIVE/DEAD® Viability/Cytotoxicity kit was purchased from Invitrogen (Carlsbad, CA). Human serum albumin was obtained from Bayer (Elkhart, IN). TGF-β1 was purchased from PeproTech, Inc. (Rocky Hill, NJ). Photoinitiator Irgacure 2959 (I-2959) was purchased from Ciba Specialty Chemicals (Tarrytown, NY). Primers were from Applied Biosystems (Carlsbad, CA). All other chemicals were obtained from Sigma-Aldrich (St. Louis, MO) unless otherwise noted.

Preparation of PEGDMA

PEGDMA (3400 MW) was synthesized as described previously.[19] Briefly, PEG (3 kDa) was dissolved in tetrahydrofuran and reacted with methacryloyl chloride in the presence of triethylamine overnight under nitrogen. Synthesized PEGDMA macromer was purified by precipitation in ethyl ether and lyophilized overnight. Methacrylation of the reaction was over 95% as determined by proton nuclear magnetic resonance (^{1}H NMR).

Human articular chondrocyte isolation

Healthy human articular cartilage was supplied by the South Texas Tissue Center (San Antonio, TX) from adult donors (mean ± SD age 35.8 ± 8.0) having no history of joint disease. Human tissues were obtained under approval by the Scripps Human Subjects Committee. Articular cartilage and chondrocytes were harvested and isolated from cadavers within 22 to 72 h after death as previously described.[20,21] Briefly, once cartilage surfaces were rinsed with sterilized phosphate buffered saline (PBS), sterile scalpels were used to excise articular cartilage from femoral condyles and tibia plateaus under aseptic conditions. Harvested cartilage samples were minced and treated with 0.5 mg/mL trypsin at 37°C for 15 min. After removing trypsin solution, the cartilage tissues were digested with 2 mg/mL type IV clostridial collagenase in DMEM with 5% fetal calf serum for 12 to16 h at 37°C.

The released human articular chondrocytes were washed three times with DMEM supplemented with 1 × penicillin–streptomycin–glutamine (PSG; Invitrogen) and cell viability was determined (average viability of 95%). Isolated chondrocytes were seeded into T175 tissue culture flasks at 5 million cells per flask for expansion in monolayer and cultured in DMEM supplemented with 10% calf serum and 1 × PSG. Cells were incubated at 37°C with humidified air containing 5% CO_2. The culture medium was changed every 4 days. Human chondrocytes were ready to use when 80% to 90% confluence was reached (1 to 2 weeks in primary culture). All cells used for this study were from first or second passage.

Three-dimensional biopaper preparation

OC plugs served as the 3D biopaper for bioprinting. Plugs were harvested from bovine femoral condyles (Animal Technologies, Tyler, TX) with 8-mm-diameter stainless steel punch under aseptic conditions. Sterile PBS was used to rinse the cartilage surface during the harvest to prevent drying. Harvested OC plugs were rinsed three times with DMEM supplemented with 1 × antibiotic–antimycotic solution (Invitrogen). A 4-mm-diameter sterile biopsy punch (Sklar Instruments, West Chester, PA) was used to make full-thickness cartilage lesion in the center of the OC plugs. Depths of the defects ranged from 2 to 5 mm depending on the thickness of cartilage. Plugs were cultured in DMEM supplemented with 10% calf serum and 1 × PSG and discarded after 2 weeks if not used. In this study, all OC plugs were used fresh on the same day of harvest. Viability and potential for healing of chondral lesions in OC plugs have been previously characterized.[22]

Bioink preparation

Purified PEGDMA was dissolved in PBS or deionized water to a final concentration of 10% and 20% weight/volume (w/v). Photoinitiator I-2959 was added at a final concentration of 0.05% w/v to provide a cytocompatible photoinitiating condition.[23] Human articular chondrocytes

were suspended in filter-sterilized PEGDMA solution at 5×10^6 cells/mL.

Green and orange fluorescent (color) bioink was prepared by labeling human chondrocytes with CellTrace Green CFSE and CellTracker Orange CMTMR fluorescent probes (Invitrogen) following protocols provided by the manufacturer. Briefly, chondrocytes were suspended in 10 μM staining solutions and incubated for 15 min at 37°C. After centrifugation, cell pellets were suspended with prewarmed DMEM and incubated for another 30 min to complete the staining. Labeled cells were suspended in PEGDMA solution to form color bioink at 5×10^6 cells/mL.

Bioprinting

The bioprinting platform based on a modified HP Deskjet 500 printer was set up as previously described.[12] The printer was sterilized using ultraviolet (UV) light for at least 2h. HP Deskjet pens with 50 firing chambers were sprayed with 70% ethanol for sterilization. A long-wave ultraviolet lamp (Model B-100AP; UVP, Upland, CA) was set up above the printing platform with a distance of 25 cm for simultaneous photopolymerization during the printing. UV intensity at the platform was 4 to 8 mW/cm^2 according to the manufacturer, and the intensity of 4.5 mW/cm^2 was further verified using a UV light meter (UV513AB; General Tools, New York City, NY). The printer pen was filled with bioink and covered by aluminum foil to protect from UV exposure. OC plugs with artificial defects or cylindrical molds with 5-mm internal diameter served as 3D biopaper. The distance between the printhead and biopaper was set at 1 to 2 mm. Patterns with the shape and size of the cartilage defect or mold were designed using Adobe Photoshop (Adobe Systems, San Jose, CA) and printed layer by layer to fabricate a 3D construct. Printed cell–hydrogel constructs were cultured with DMEM supplemented with 1 × insulin–transferrin–selenium (ITS+), 0.1 mM ascorbic acid 2-phosphate, 1.25 mg/mL human serum albumin, 10^{-7} M dexamethasone, 1 × PSG, and 10 ng/mL TGF-β1 to maintain chondrogenic phenotype of chondrocytes[24] for 2, 4, and 6 weeks. The medium was changed every 3 days. Cell viability was measured with Live/Dead Viability/Cytotoxicity assay 24 h after printing.

Color bioink formulated with fluorescently labeled chondrocytes was printed to fabricate zonal layers to demonstrate the feasibility of fabricating cartilage zonal structure. A Zeiss LSM 510 laser scanning confocal microscope (Carl Zeiss, Minneapolis, MN) was used to determine the cell and scaffold deposition in 3D with appropriate channels at 488 and 543 nm for the fluorescence.

Mechanical characterization of printed PEGDMA hydrogels

A customized electromechanical testing system with a 50-g load cell (LSB200; Futek, Irvine, CA) and a dual-axis controller (LAC-25; SMAC, Carlsbad, CA) was employed to measure the compressive modulus of prepared PEGDMA hydrogels at room temperature. Acellular hydrogels were allowed to swell to equilibrium in DMEM for 48 h at 37°C before testing. The hydrogel samples were placed in a parallel-plate configuration, and the thickness of hydrogel was measured by the axis controller. The hydrogel was compressed in a step-wise manner to a maximum of 20% compressive strain with four progressive strain loadings with a test velocity of 0.1 mm/s. Each loading cycle was followed by a relaxation phase to sample equilibrium. The unconfined equilibrium compressive modulus was determined from the slope of the stress–strain curve obtained from the load and displacement data at the end of each relaxation phase.[25] A sample size of three was used for each condition.

Swelling studies of printed PEGDMA hydrogels

Printed PEGDMA hydrogels were allowed to swell to equilibrium in the culture medium at 37°C for 48 h before weighing to obtain equilibrium swollen mass. Dry mass was obtained by lyophilizing hydrogels for 48 h. The equilibrium mass swelling ratio (Q) and water content (M) of hydrogel constructs were determined by the following equations.

$$\text{Mass swelling ratio } Q = \frac{W_s}{W_d}$$

$$\text{Equilibrium water content } M = \frac{W_s - W_d}{W_s} \times 100\%$$

Here, W_s and W_d represent the weight of hydrogel construct after equilibrium swelling in the culture medium, and the dry weight of lyophilized hydrogel construct, respectively.

RNA isolation and gene expression using quantitative real-time polymerase chain reaction

Cell–hydrogel constructs were harvested and analyzed for gene expression at 2, 4, and 6 weeks of culture ($n=3$). Samples were frozen immediately in liquid nitrogen and pulverized with a biopulverization kit. Pulverized powder was carefully collected into a tube containing RNA lysis buffer provided by RNeasy Mini Kit (QIAGEN, Valencia, CA) and incubated at room temperature for 10 min. The lysed solution was transferred into shredder tubes (QIAGEN) and centrifuged at 12,000 *g* for 2 min. The homogenized solution was then transferred to spin tubes and RNA was purified following the protocol provided with the kit. Total RNA content and purity was quantified using the Nanodrop ND-1000 (Thermo Scientific, Wilmington, DE). Isolated total RNA was reverse transcribed to cDNA using a High Capacity cDNA Reverse Transcription Kit (Applied Biosystems) following the kit protocol. Quantitative real-time polymerase chain reaction (RT-PCR) (LightCycler 480II Real-Time PCR System, Roche, Basel, Switzerland) was performed using TaqMan Gene Expression Assay probes (Applied Biosystems) to determine the gene expression of human collagen type I (*COL1A1*; Hs00164004_m1), collagen type II (*COL2A1*; Hs01064869_m1), and aggrecan (*ACAN*; Hs00153936_m1) relative to the expression of glyceraldehyde-3-phosphate dehydrogenase (*GAPDH*; Hs99999905_m1). *GAPDH* was used as housekeeping gene for normalization.

Biochemical assays

Cell–hydrogel constructs collected at different time point were lyophilized for at least 48 h before cell lysis. Lyophilized constructs were sliced into small pieces with scalpels and digested with papain or pepsin. Total glycosaminoglycan (GAG) content was extracted by treating each sample with 1 mL papain solution (125 μg/mL papain type III (Worthington Biochemical, Lakewood, NJ), 10 mM l-cysteine,

100 mM phosphate buffer, and 10 mM EDTA, pH 6.4) for 16 h at 60°C. Soluble collagen was extracted by digesting each sample with 1 mL pepsin solution (100 μg/mL pepsin in 0.05 M acetic acid) for 6 days at 4°C to avoid denaturation.

DNA content in each sample was measured using CyQUANT Cell Proliferation Assay (Invitrogen) following the kit protocol. Results were measured using a TECAN Safire 2 microplate reader (Mannedorf, Switzerland). Total GAG content was determined with dimethymethylene blue dye assay.[26] Solubilized type I and type II collagen were measured with ELISA detection kits (#6008, #6009, Chondrex, Redmond, WA) following the protocol provided by the manufacturer. GAG, type I, and type II collagen contents were normalized to respective DNA content to assess biosynthetic activity of embedded human chondrocytes. A sample size of three was used.

Histology

Cell–hydrogel constructs were fixed overnight in 10% formaldehyde and transferred to 70% ethanol until embedded in paraffin following standard histological protocol. OC plugs were decalcified with Shandon TBD-2 decalcifier (Thermo Scientific, Logan, UT) for 4 days after fixation. After embedding in paraffin, samples were microtomed (Microm HM 325, GMI Inc., Ramsey, MN) into 6-μm cross sections. Representative sections of each construct were stained with Safranin-O/fast green to visualize proteoglycans secreted in the hydrogels.

Interface failure stress

PEG hydrogel with cells were printed into the defect of OC plugs with simultaneous photopolymerization. Samples were collected at week 2, 4, and 6 during the culture. The strength of the native/printed tissue interface was assessed by a mechanical push-out test as previously described.[22] Briefly, the chondral portions of the OC plugs with implant were carefully separated from the subchondral bone. The resulting cartilage specimen was placed in a custom holding chamber, which supported the outer ring portion of the cut tissue. The core was pushed out with a plunger slightly less than the core diameter (3.5 mm) powered by a moving coil actuator (SMAC) at a rate of 0.1 mm/s. Axial force was measured and recorded during the testing at 1 kHz. The thickness of the central core was determined with a digital caliper. The peak force measured during the test was normalized by the lateral area of the core (thickness times circumference), and the resulting value was considered the interface failure stress. A sample size of three in each group at each time point was used.

Statistical analysis

All data in this article are reported as mean with standard deviation. Statistical analysis was performed with GraphPad Prism software (Version 5; GraphPad Software, Inc., La Jolla, CA). Statistical significance was determined using one-way analysis of variance followed by Tukey's *post hoc* test with a confidence level of 0.05.

Results

Bioprinted PEGDMA hydrogel with human chondrocytes

To mimic cartilage defects, we created a 4-mm-diameter full-thickness cartilage lesion in the center of an OC plug (3D biopaper) (Figs. 1 and 2A). A polymerizable bioink was prepared by combing a PEGDMA with a photoinitiator and a suspension of human articular chondrocytes labeled with either green or orange fluorescent dyes. A modified HP Deskjet 500 was used at 300 dpi with individual ink drop volume of 130 pL. There are 50 nozzles in each printhead with a firing frequency of 3600 Hz.[27,28] Therefore, for a representative defect of 4-mm diameter and cartilage thickness of 2 mm, a nominal 0.23 μL of bioink estimated to contain 1140 human chondrocytes (5×10^6 cells/mL) was printed and photopolymerized for each layer to repair the cartilage defect in a layer-by-layer assembly. The thickness of each printed layer was about 18 μm. Total firing time of printhead was 1.1 s and the whole printing process completed in 108 s. Compared to manual hydrogel polymerization for cartilage fabrication, which requires at least 10 min for UV exposure, bioprinting reduced UV exposure to cells by more than 80%. The viability of human chondrocytes printed with simultaneous photopolymerization was 89.2 ± 3.6% ($n = 3$), compared to cell viability of 63.2 ± 9.0% ($n = 3$) when exposed to the same UV light source continuously for 10 min in PEGDMA for manual fabrication. The printed PEG gel remained bound firmly to the native tissue in the defect even after sectioning (Fig. 2B).

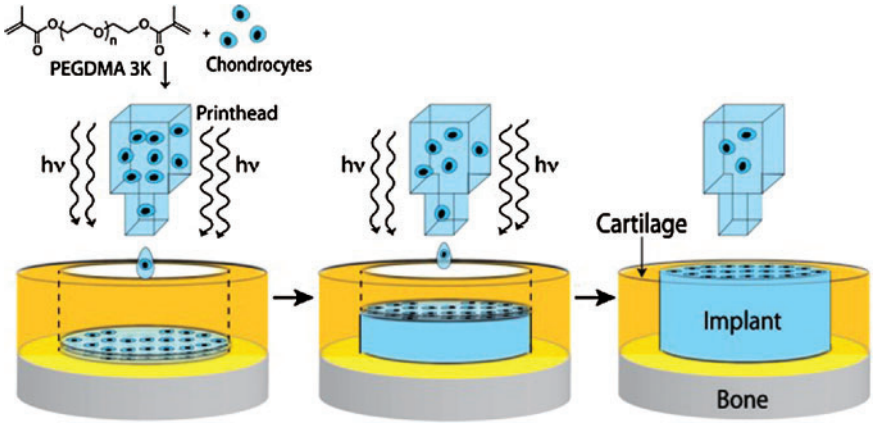

FIG. 1. Schematic of bioprinting cartilage with simultaneous photopolymerization process. PEGDMA, poly(ethylene glycol) dimethacrylate; hv, UV light energy. Color images available online at www.liebertonline.com/tea

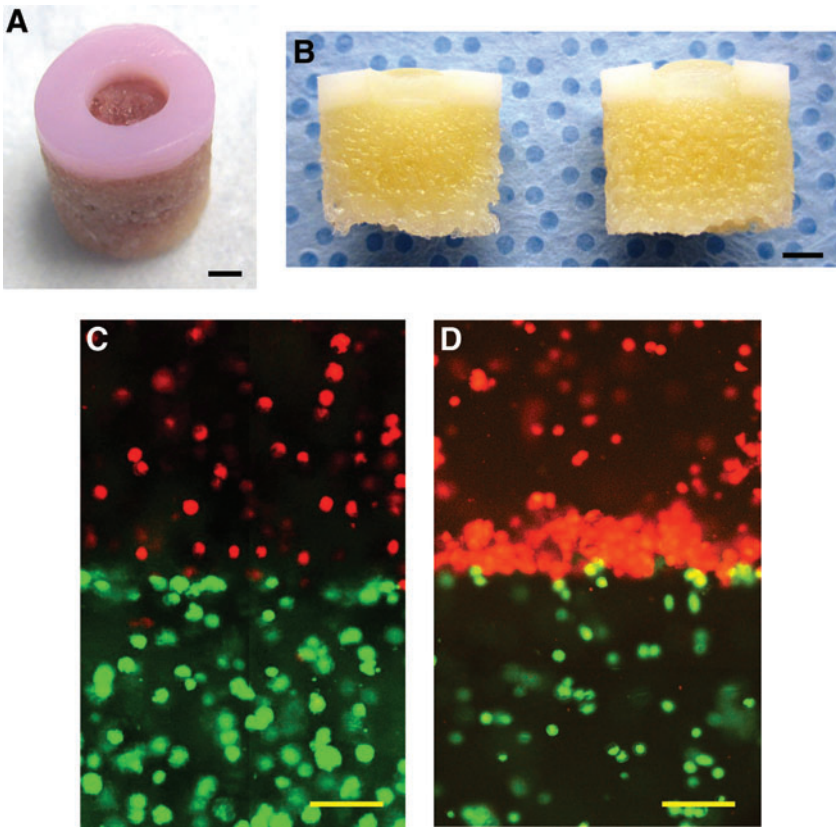

FIG. 2. OC plug (3D biopaper) and 3D distribution of printed human chondrocytes in PEG gel. **(A)** An OC plug with full-thickness cartilage lesion 4 mm in diameter and 2 mm in depth. **(B)** Decalcified OC plug cut in half with printed hydrogel in the defect. **(C)** Printed cells maintained deposited positions with simultaneous photopolymerization in layer-by-layer assembly for multiple zonal cartilage printing. Bioink with different colors was printed in layers. **(D)** Cells accumulated to the interface of the mimicked cartilage zonal structure due to gravity when polymerized after cell deposition. Scale bars: **(A, B)** = 2 mm; **(C, D)** = 100 μm. PEG, poly(ethylene glycol); OC, osteochondral; 3D, three-dimensional. Color images available online at www.liebertonline.com/tea

Figure 2C shows that an even distribution of printed human chondrocytes was obtained in the 3D PEGDMA hydrogel with simultaneous polymerization during printing. In contrast, when photopolymerization was performed after printing, the deposited chondrocytes accumulated at the zonal interface instead of their originally deposited positions due to gravity (Fig. 2D). This accumulation of cells at zonal interfaces was also observed in previous reports of manually fabricating zonal cartilage.[29,30]

Swelling and mechanical properties of printed PEGDMA scaffolds

No significant difference was observed in the swelling and equilibrium water content between printed and nonprinted PEGDMA hydrogels (both 10% and 20% w/v), as well as between hydrogels with and without cells. Doubling the concentration of PEGDMA (from 10% to 20%) increased the compressive stiffness nearly 10-fold (Table 1). Hydrogels containing cells were ~20% more flexible by this measure, presumably because the embedded chondrocytes partially absorb the loading force and perhaps because the PEGDMA photopolymerization was affected. Printing 20% w/v PEGDMA reduced compressive modulus by 18% compared to nonprinted PEGDMA (13% reduction for printed hydrogel with cells). The water content, swelling ratio, and compressive modulus of 20% w/v PEGDMA with human chondrocytes were close to the range of the properties reported for native human articular cartilage (~80% water content, 500–1000 kPa compressive

Table 1. Properties of Printed and Nonprinted Poly(Ethylene Glycol) Dimethacrylate With and Without Human Chondrocytes (n = 3)

	% (w/v) PEGDM	*Q*[a]	*M*[b] *(%)*	*Compressive modulus (kPa)*
Printed	10	12.54 ± 0.30	92.02 ± 0.19	37.75 ± 7.18
	10 (w/cells[c])	11.80 ± 0.07	91.53 ± 0.05	30.14 ± 4.41
	20	6.19 ± 0.10	83.85 ± 0.26	395.73 ± 80.40
	20 (w/cells)	6.10 ± 0.05	83.60 ± 0.14	321.06 ± 43.99
Nonprinted	10	12.18 ± 0.01	91.74 ± 0.06	47.61 ± 2.80
	10 (w/cells)	12.51 ± 0.04	92.00 ± 0.03	36.12 ± 8.44
	20	6.68 ± 0.15	85.04 ± 0.34	483.75 ± 29.47
	20 (w/cells)	6.75 ± 0.10	85.19 ± 0.23	372.40 ± 37.85

[a]Mass–swelling ratio.
[b]Equilibrium water content.
[c]Human chondrocytes concentration in hydrogels: 5×10^6 cells/mL.
w/v, weight/volume; PEGDMA, poly(ethylene glycol) dimethacrylate.

modulus),[31] and so this formulation was selected for further study.

Gene expression of printed human chondrocytes

The expression of human collagen type I, collagen type II, and aggrecan genes was measured using quantitative PCR, normalizing to the *GAPDH* housekeeping gene. To determine the effect of co-culture in OC plugs, relative gene expression of target genes was normalized to expression levels in PEG gel printed in plastic molds without OC plugs, and cultured for 2 weeks. The results of these studies are shown in Figure 3.

Collagen type II expression increased significantly from week 2 to week 6 for both groups during the culture (Fig. 3A). Printed cartilage implants in 3D biopaper had significantly higher collagen type II and aggrecan expression than those printed in plastic molds at all time points (Fig. 3A, B). The average collagen type II and aggrecan expression of printed cartilage tissue in 3D biopaper was ~72% and 48% greater than cell–hydrogel constructs without biopaper cultured for 6 weeks. Collagen type I expression decreased significantly for both groups from week 2 to 6 (Fig. 3C).

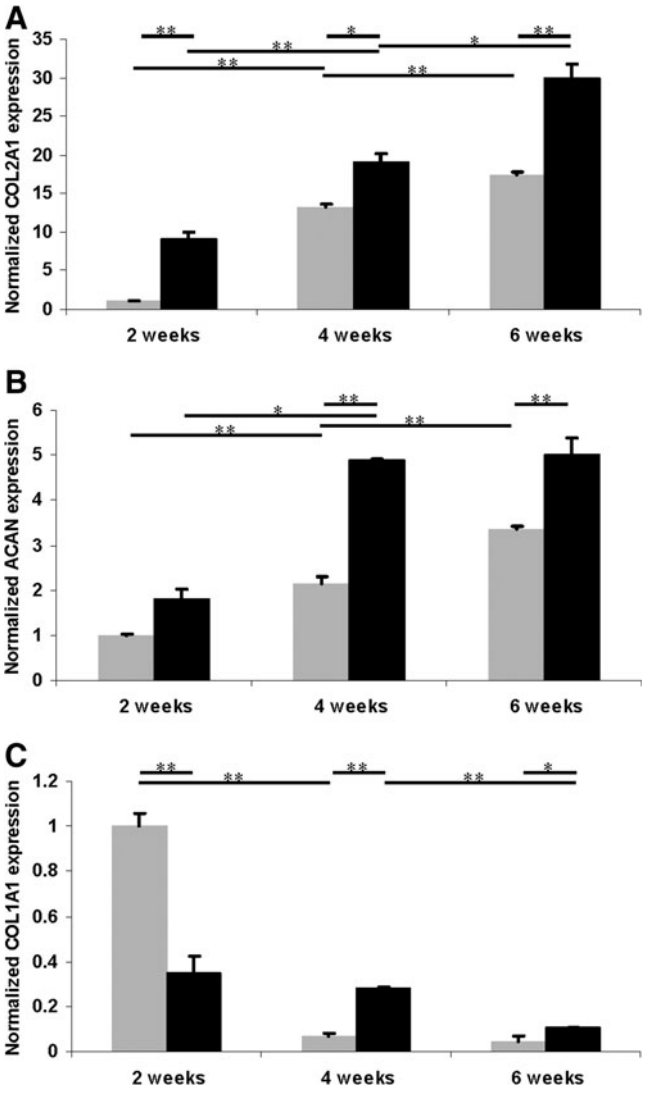

FIG. 3. Gene expression in human chondrocytes embedded in PEG hydrogel with (black bars) and without (grey bars) OC plug cultured for 2, 4, and 6 weeks (normalized to 2 week expression without OC plug). **(A)** Collagen type II expression. **(B)** Aggrecan expression. **(C)** Collagen type I expression. Asterisks indicate statistical significance between assigned groups (*$p < 0.05$; **$p < 0.01$) ($n = 3$).

Biochemical analysis of printed tissue constructs

ECM production by the printed cells—the first step in neocartilaginous tissue formation—was evaluated by measuring the amounts of ECM components GAG and collagen type II, normalized to the DNA content of each sample, as shown in Figure 4. The GAG/DNA content was significantly higher than the collagen type II/DNA content in both groups, similar to other reports of *in vitro* culture of chondrocytes in PEG hydrogel.[16,32] GAG and collagen type II production of printed cartilage in OC plugs increased significantly from 2 to 4 weeks in culture, and then leveled out, whereas the amounts of GAG and collagen type II produced in cell–hydrogel constructs in plastic molds increased throughout the experiment. The average GAG/DNA production of chondrocytes cultured without OC plugs was only 50% of that in the implant cultured with OC plugs at week 6, which is consistent with the gene expression data. Collagen type I content was undetectable at all time points

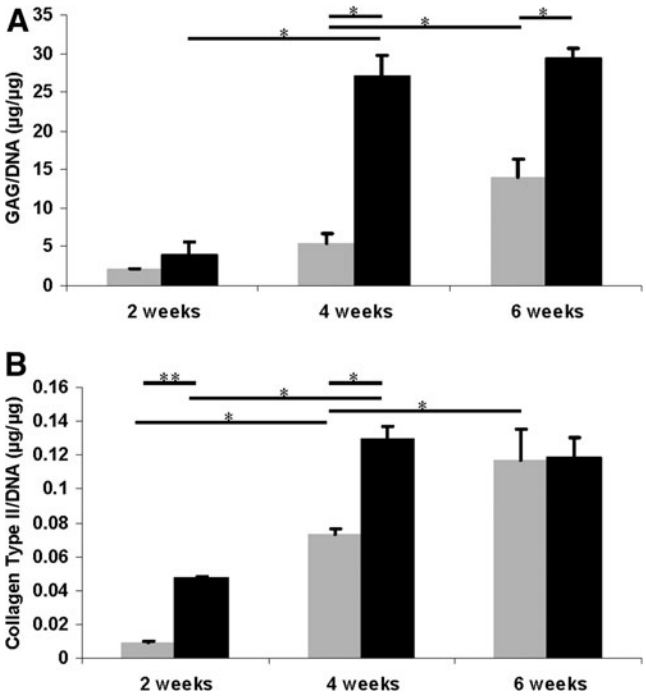

FIG. 4. ECM production normalized to DNA content of human chondrocytes embedded in PEG hydrogel with (black bars) and without (gray bars) OC plug cultured for 2, 4, and 6 weeks. **(A)** GAG production normalized to DNA content (μg/μg). **(B)** Soluble collagen type II production normalized to DNA content (μg/μg). Asterisks indicate statistical significance between assigned groups (*$p < 0.05$; **$p < 0.01$) ($n = 3$). ECM, extracellular matrix; GAG, glycosaminoglycan.

using ELISA demonstrated the recovered chondrogenic phenotype since week 2 in 3D culture.

Integration of printed hydrogels into OC plug

Evidence of full stabilization and integration of the printed neocartilage construct in the defect of OC plugs after 6 weeks in culture is shown in Figure 5A. The hydrogel containing cells remained firmly attached to the surrounding cartilage as well as the subchondral bone (Fig. 5B, C). Safranin-O staining revealed greater proteoglycan production at the interface between printed cell-laden hydrogel and native cartilage of biopaper. These results contrast with those of previous studies, which described no ECM formation in acellular PEG hydrogel adhered with native cartilage.[33] This indicates that direct printing for cartilage repair to the native cartilage enhanced tissue integration and ECM production. Human chondrocytes encapsulated hydrogel cultured without OC plug had overall lower proteoglycan production (Fig. 5D).

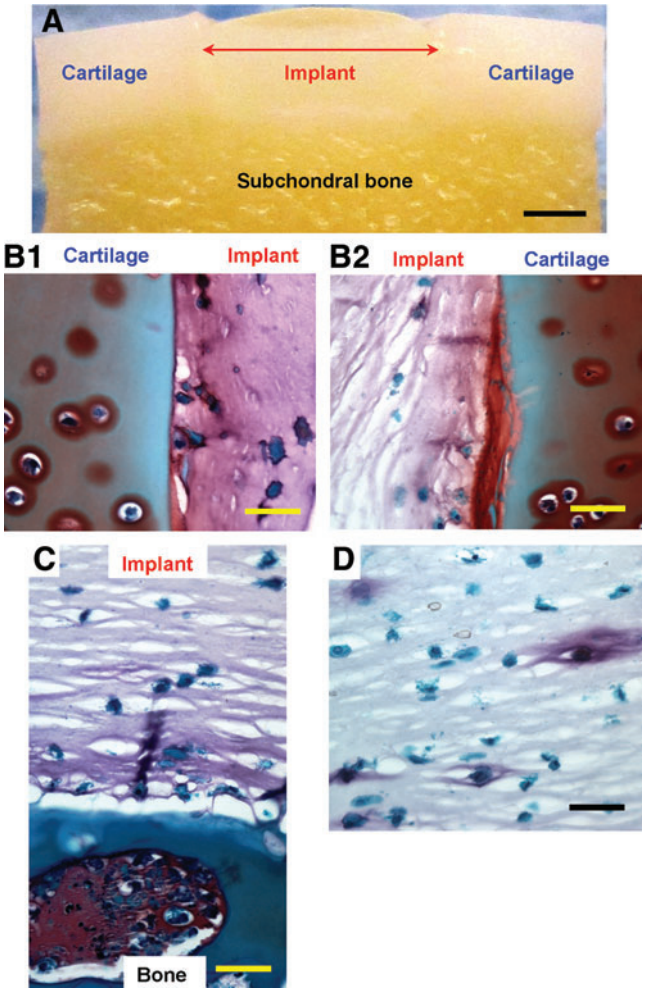

FIG. 5. Integration of printed hydrogels to the 3D biopaper (OC plug) after 6 weeks in culture. **(A)** Light microscopy image of PEG hydrogel printed in the defect of an OC plug. **(B, D)** Safranin-O staining of printed cell-laden hydrogel, in which proteoglycans are stained red-purple. **(B1, B2)** Two halves of cross-sectional slice showing proteoglycan production through the implant material and especially at the implant–cartilage interface. **(C)** Slice through implant material and bone showing good integration between subchondral bone and implant with ECM at the interface. **(D)** Safranin-O staining of hydrogel with embedded human chondrocytes cultured for 6 weeks without OC plug showing significantly less and more localized production of proteoglycan. Scale bars: **(A)** = 2 mm; **(B–D)** = 200 μm. Color images available online at www.liebertonline.com/tea

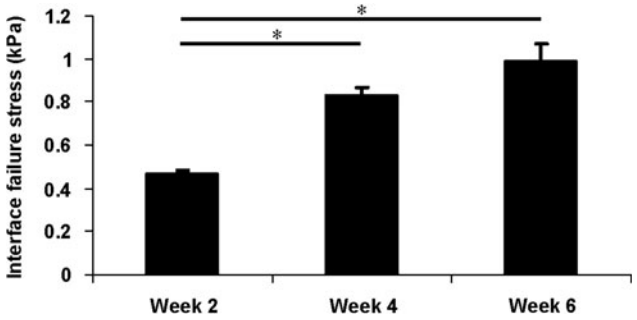

FIG. 6. Native/engineered tissue interface stress assessed by push-out testing. PEG hydrogel with human chondrocytes were printed to repair the defects in OC plugs. Samples were collected at week 2, 4, and 6 during the culture for push-out testing. Asterisks indicate statistical significance between assigned groups ($*p < 0.05$) ($n = 3$).

The interface failure strength increased steadily with time during the culture (Fig. 6). At week 4 and 6, the integration was significantly higher than the stress initially measured at week 2 ($p < 0.05$). The interface failure strength measured at week 6 was also greater than the stress measured at week 4 although it was not statistically significant ($p = 0.063$). These data are consistent with the histology observations.

Discussion

This 3D thermal inkjet-based bioprinting/photopolymerization method provides the first example of computer-controlled layer-by-layer construction of material with sufficient mechanical stability for cartilage development. Significantly greater resolution is obtained here (85 μm with an 18-μm-layer thickness) than the best previously reported method of *in situ* printing of OC defects using syringe-extruded acellular alginate hydrogel (800 μm resolution).[34] Better printing resolution is particularly attractive for the repair of the articular cartilage superficial zone, which is only about 200 μm thick and almost impossible to repair manually.[35] Furthermore, simultaneous polymerization during 3D printing is critical to the maintenance of precise positions of deposited cells and biomaterial scaffolds during layer-by-layer assembly. Microfabrication with each printed layer also resulted in smoother transitions between zonal layers, reducing the potential for degradation due to delamination. By adjusting these bioprinting parameters as well as the components of the bioink, we believe that we will be able to construct the kind of complex 3D structures required to heal a wide variety of cartilaginous lesions.

Although the compressive modulus of printed PEGDMA gel was 18% lower than manually fabricated PEGDMA gel, it was still within the range of modulus of native human articular cartilage.[31] The lower compressive modulus of printed PGEDMA may due to the shorter photopolymerization

time as well as the possible lower degree of integration between multiple printed layers. Nevertheless, the PEGDMA hydrogels provided a biocompatible environment for human chondrocytes, indicated by the maintenance of cell viability, phenotype, and biosynthetic function. Collagen type II and aggrecan are the primary components in articular cartilage ECM (50%–90% dry weights),[36] whereas collagen type I production indicates de-differentiation of chondrocytes and is a marker of fibrocartilage formation.[37] We found collagen type II and aggrecan gene expression of printed cell–hydrogel constructs in OC plugs to be significantly higher than those without OC plugs after 6 weeks of cell culture. Decreased collagen type I expression in both groups from week 2 to 6 demonstrated that embedded chondrocytes maintained chondrogenic phenotype in 3D hydrogels during the culture.

Biochemical analysis also showed increase in GAG and collagen type II production in both groups during the culture. GAG/DNA production in chondrocytes cultured with OC plugs was significantly higher than that in the implant cultured without OC plugs at week 6. At week 4, both GAG/DNA and collagen type II/DNA production of chondrocytes cultured with OC plugs was significantly higher than those in the implant cultured without OC plugs. These results were consistent with the gene expression data. Thus, all indications were consistent with the conclusion that the native cartilage surrounding the implant has a positive effect on chondrogenesis in the engineered tissue, as well as on accelerated ECM production.

One of the major challenges in articular cartilage tissue engineering is the stabilization of the implanted biomaterial scaffold in the joint as well as the integration between the implant and surrounding native tissue. Suturing or gluing implants to the cartilage defects is technically demanding and does not yield consistent clinical results.[4] New cartilage defects created by sutures or tacks persist in the tissue permanently.[4] Overall, the printed hydrogel-stabilized neocartilage described here demonstrated excellent integration with the surrounding native cartilage and bone tissue. The more extensive ECM production observed at the interface between the hydrogel scaffold and the host cartilage revealed the importance of the remaining cartilage tissue at lesion site in promoting neocartilage formation in implanted cell–hydrogel constructs. This histology observation was further supported by the interface failure stress between the printed implant and the native cartilage assessed by mechanical push-out testing. The interface failure stress increased significantly in the samples from week 2 to 6 revealed the enhanced ECM deposition and phenotype maturation in the printed neocartilage with native tissue. Therefore, the direct micro-printing process has the potential of fabricating the repaired tissue with enhanced integration to the lesion site. By using 3D reconstructions of scanned lesions, bioprinting is able to precisely deliver cells, growth factors, and biomaterial scaffolds to repair the cartilage lesion with various shapes and thickness with digital control.

In conclusion, this work demonstrates the feasibility of fabricating anatomic cartilage structures by delivering chondrocytes and biomaterial scaffold to precise target locations in 3D for zonal cartilage engineering. PEGDMA with human chondrocytes was continuously bioprinted for direct cartilage repair using layer-by-layer assembly. Simultaneous photopolymerization maintained the printed cells at the initially deposited positions and reduced phototoxicity. Printed cell-laden hydrogel firmly integrated with native tissue in 3D biopaper maintaining cell phenotype with consistent gene expression analysis and biochemical data. The presence of native cartilage promoted ECM production by the encapsulated human chondrocytes and enhanced proteoglycan deposition was observed at the interface between printed biomaterial and native cartilage. Therefore, bioprinting based on thermal inkjet printing technology can be a promising approach for anatomic cartilage engineering.

Acknowledgments

The authors would like to acknowledge Melissa Szeto for harvesting human chondrocytes; Jonathan Netter and Nick Steklov for assisting with mechanical testing; William Hui, Margaret Chadwell, and Lilo Creighton for helping with histology; and Chien-Chi Lin, Shawn Grogan, Noboru Taniguchi, Stuart Duffy, Sujata Sovani, Chantal Pauli, Marissa Chen, Diana Brinson, and Olee Tsaiwei for constructive suggestions and other technical support. This work was funded by the NIH (AG007996), CIRM (TR1-01216), STSI (UL1 RR025774), and NSF (grant no.1011796).

Disclosure Statement

The authors certify that there is no conflict of interest related to the work presented in this article.

References

1. Mow, V.C., and Hayes, W.C. Basic Orthopaedic Biomechanics. Philadelphia: Lippincott Williams & Wilkins, 1997.
2. Rasanen, P., Paavolainen, P., Sintonen, H., Koivisto, A.M., Blom, M., Ryynanen, O.P., *et al.* Effectiveness of hip or knee replacement surgery in terms of quality-adjusted life years and costs. Acta Orthop **78,** 108, 2007.
3. Brittberg, M., Lindahl, A., Nilsson, A., Ohlsson, C., Isaksson, O., and Peterson, L. Treatment of deep cartilage defects in the knee with autologous chondrocyte transplantation. N Engl J Med **331,** 889, 1994.
4. Hunziker, E.B. Articular cartilage repair: basic science and clinical progress. A review of the current status and prospects. Osteoarthritis Cartilage **10,** 432, 2002.
5. Kalson, N.S., Gikas, P.D., and Briggs, T.W. Current strategies for knee cartilage repair. Int J Clin Pract **64,** 1444, 2010.
6. Shapiro, F., Koide, S., and Glimcher, M.J. Cell origin and differentiation in the repair of full-thickness defects of articular-cartilage. J Bone Joint Surg Am **75A,** 532, 1993.
7. Mohebi, M.M., and Evans, J.R.G. A drop-on-demand ink-jet printer for combinatorial libraries and functionally graded ceramics. J Comb Chem **4,** 267, 2002.
8. Hock, S.W., Johnson, D.A., and Van Veen, M.A. US Patent 5521622. 1996.
9. Canfield, B., Clayton, H., and Yeung, K.W.W. US Patent 5673069. 1997.
10. Hudson, K.R., Cowan, P.B., and Gondek, J.S. US Patent 6042211. 2000.
11. Cui, X., Dean, D., Ruggeri, Z.M., and Boland, T. Cell damage evaluation of thermal inkjet printed Chinese hamster ovary cells. Biotechnol Bioeng **106,** 963, 2010.
12. Cui, X., and Boland, T. Human microvasculature fabrication using thermal inkjet printing technology. Biomaterials **30,** 6221, 2009.

13. Deitch, S., Kunkle, C., Cui, X., Boland, T., and Dean, D. Collagen matrix alignment using inkjet printer technology. Mater Res Soc Symp Proc **1094,** 52, 2008.
14. Boland, T., Xu, T., Damon, B., and Cui, X. Application of inkjet printing to tissue engineering. Biotechnol J **1,** 910, 2006.
15. Xu, T., Gregory, C.A., Molnar, P., Cui, X., Jalota, S., Bhaduri, S.B., and Boland, T. Viability and electrophysiology of neural cell structures generated by the inkjet printing method. Biomaterials **27,** 3580, 2006.
16. Elisseeff, J., McIntosh, W., Anseth, K., Riley, S., Ragan, P., and Langer, R. Photoencapsulation of chondrocytes in poly(ethylene oxide)-based semi-interpenetrating networks. J Biomed Mater Res **51,** 164, 2000.
17. Bryant, S.J., and Anseth, K.S. Hydrogel properties influence ECM production by chondrocytes photoencapsulated in poly(ethylene glycol) hydrogels. J Biomed Mater Res **59,** 63, 2002.
18. Bryant, S.J., Chowdhury, T.T., Lee, D.A., Bader, D.L., and Anseth, K.S. Crosslinking density influences chondrocyte metabolism in dynamically loaded photocrosslinked poly(ethylene glycol) hydrogels. Ann Biomed Eng **32,** 407, 2004.
19. Lin-Gibson, S., Bencherif, S., Cooper, J.A., Wetzel, S.J., Antonucci, J.M., Vogel, B.M., *et al.* Synthesis and characterization of PEG dimethacrylates and their hydrogels. Biomacromolecules **5,** 1280, 2004.
20. Maier, R., Ganu, V., and Lotz, M. Interleukin-11, an inducible cytokine in human articular chondrocytes and synoviocytes, stimulates the production of the tissue inhibitor of metalloproteinases. J Biol Chem **268,** 21527, 1993.
21. Blanco, F.J., Ochs, R.L., Schwarz, H., and Lotz, M. Chondrocyte apoptosis induced by nitric-oxide. Am J Pathol **146,** 75, 1995.
22. Tam, H.K., Srivastava, A., Colwell, C.W., and D'Lima, D.D. *In vitro* model of full-thickness cartilage defect healing. J Orthop Res **25,** 1136, 2007.
23. Bryant, S.J., Nuttelman, C.R., and Anseth, K.S. Cytocompatibility of UV and visible light photoinitiating systems on cultured NIH/3T3 fibroblasts *in vitro*. J Biomater Sci Polym Ed **11,** 439, 2000.
24. Schmitt, B., Ringe, J., Haupl, T., Notter, M., Manz, R., Burmester, G.R., *et al.* BMP2 initiates chondrogenic lineage development of adult human mesenchymal stem cells in high-density culture. Differentiation **71,** 567, 2003.
25. Hoenig, E., Winkler, T., Mielke, G., Paetzold, H., Schuettler, D., Goepfert, C., *et al.* High amplitude direct compressive strain enhances mechanical properties of scaffold-free tissue-engineered cartilage. Tissue Eng Part A **17,** 1401, 2011.
26. Farndale, R.W., Buttle, D.J., and Barrett, A.J. Improved quantitation and discrimination of sulfated glycosaminoglycans by use of dimethylmethylene blue. Biochim Biophys Acta **883,** 173, 1986.
27. Harmon, J.P., and Widder, J.A. Integrating the printhead into the HP Deskjet printer. Hewlett-Packard J **39,** 62, 1988.
28. Buskirk, W.A., Hackleman, D.E., Hall, S.T., Kanarek, P.H., Low, R.N., Trueba, K.E., *et al.* Development of a high-resolution thermal inkjet printhead. Hewlett-Packard J 3**9,** 55, 1988.
29. Kim, T.K., Sharma, B., Williams, C.G., Ruffner, M.A., Malik, A., McFarland, E.G., *et al.* Experimental model for cartilage tissue engineering to regenerate the zonal organization of articular cartilage. Osteoarthritis Cartilage **11,** 653, 2003.
30. Sharma, B., Williams, C.G., Kim, T.K., Sun, D.N., Malik, A., Khan, M., *et al.* Designing zonal organization into tissue-engineered cartilage. Tissue Eng **13,** 405, 2007.
31. Armstrong, C.G., and Mow, V.C. Variations in the intrinsic mechanical proterties of human articular-cartilage with age, degeneration, and water-content. J Bone Joint Surg Am **64,** 88, 1982.
32. Elisseeff, J., Anseth, K., Sims, D., McIntosh, W., Randolph, M., Yaremchuk, M., *et al.* Transdermal photopolymerization of poly(ethylene oxide)-based injectable hydrogels for tissue-engineered cartilage. Plast Reconstr Surg **104,** 1014, 1999.
33. Wang, D.A., Varghese, S., Sharma, B., Strehin, I., Fermanian, S., Gorham, J., *et al.* Multifunctional chondroitin sulphate for cartilage tissue-biomaterial integration. Nat Mater **6,** 385, 2007.
34. Cohen, D.L., Lipton, J.I., Bonassar, L.J., and Lipson, H. Additive manufacturing for *in situ* repair of osteochondral defects. Biofabrication **2,** 035004, 2010
35. Hunziker, E.B., Quinn, T.M., and Hauselmann, H.J. Quantitative structural organization of normal adult human articular cartilage. Osteoarthritis Cartilage **10,** 564, 2002.
36. Muir, H. The Chondrocyte, Architect of Cartilage—Biomechanics, Structure, Function and Molecular-Biology of Cartilage Matrix Macromolecules. Bioessays **17,** 1039, 1995.
37. Benya, P.D., Padilla, S.R., and Nimni, M.E. Independent regulation of collagen types by chondrocytes during the loss of differentiated function in culture. Cell **15,** 1313, 1978.

Address correspondence to:
Darryl D. D'Lima, M.D., Ph.D.
Department of Molecular and Experimental Medicine
The Scripps Research Institute
10550 North Torrey Pines Road
La Jolla, CA 92037

E-mail: ddlima@scripps.edu

Received: September 26, 2011
Accepted: February 29, 2012
Online Publication Date: April 18, 2012